Desalination and Water Treatment
www.deswater.com

doi: 10.1080/19443994.2014.933043

53 (2015) 3388–3396
March

Taylor & Francis
Taylor & Francis Group

The effect of fast mixing conditions on the coagulation–flocculation process of highly turbid suspensions using liquid bittern coagulant

Sara BinAhmed[a,*], Georges Ayoub[a], Mahmoud Al-Hindi[b], Fouad Azizi[b]

[a]*Department of Civil and Environmental Engineering, American University of Beirut, Riad El-Solh, Beirut 1107 2020, Lebanon, emails: binahmed.sara@gmail.com (S. BinAhmed), gayoub@aub.edu.lb (G. Ayoub)*
[b]*Chemical Engineering Program, American University of Beirut, Riad El-Solh, Beirut 1107 2020, Lebanon, emails: ma211@aub.edu.lb (M. Al-Hindi), fa48@aub.edu.lb (F. Azizi)*

Received 11 October 2013; Accepted 5 February 2014

ABSTRACT

The effect of fast mixing on floc formation and pollutant removal, using magnesium hydroxide as a coagulant, was investigated through characterization of relative strength and size of the formed flocs while operating at different mixing speeds and mixing times using a dynamic optical monitoring apparatus, and photometric dispersion analyzer (PDA2000). The parameters investigated included fast mixing speed (80, 100, and 120 rpm) and time (20, 40, and 60 s). Highly turbid kaolin clay suspensions (1213 ± 36 NTU) were alkalized using sodium hydroxide (NaOH) to pH values of 10.51 ± 0.02 at temperatures 20.7 ± 0.1 °C, and liquid bittern (LB) was used as a coagulant. Fast mixing time had a clear effect on the flocs resistance to applied shear during the slow mixing phase. For all fast mixing times, 120 rpm caused the formation of largest flocs. Stronger flocs, indicated by the least change in flocculation index with time, required 60 s to form at all fast mixing speeds. Turbidity and TSS removal efficiencies are not only dependent on fast mixing speed but also on fast mixing time, such that higher fast mixing speeds were required for shorter mixing times

Keywords: Coagulation; Flocculation; Liquid bittern; Fast mixing speed; Fast mixing time

---

1. Introduction

Many industries, such as water and wastewater treatment (WWT) and materials processing, depend on separating the suspended and colloidal particles from the liquid phase using a process which involves coagulation/flocculation in most cases. The flocs formed from the most widespread processes of coagulation–flocculation are removed by “sedimentation, filtration, and/or centrifugation” [1–4]. The size and structure of the flocs are key parameters in determining the efficiency of the solid/liquid separation processes such that “large and compact” are considered optimal characteristics ensuring faster settling of denser flocs [1,4–7]. The success of the coagulation–flocculation process depends on various factors, such as temperature, alkalinity, pH, coagulant nature and dose, applied shear especially in the rapid mixing phase, and particle concentration [2,8–11]. So, varying any of the operating condition is expected to change the properties of the primary particles formed during

---

*Corresponding author.

Presented at the International Conference WIN4Life, 19–21 September 2013, Tinos Island, Greece

coagulation and, consequently, the properties of the final floc [12].

During coagulation, cations are added as coagulants at corresponding pH and dosage to treat water, thus, disturbing the existing stability due to the repulsive forces between the negatively charged colloidal particles in water [6]. The commonly used cations are Fe^{3+} and Al^{3+}, yet, another effective cation that can act as a coagulant and adsorbent in the chemical treatment of domestic and industrial wastewaters is the magnesium ion (Mg^{2+}). The main coagulation mechanism of Mg^{2+} is the precipitation of magnesium hydroxide $MgOH_2$) at pH values greater than 10.5, such that colloidal particles are removed by adsorption onto the gelatinous $MgOH_2$ floc. An abundant and cheap source of Mg^{2+} ions are the magnesium sulfate ($MgSO_4$) and magnesium chloride ($MgCl_2$) salts present in seawater. A viscous liquid called liquid bittern (LB), containing "high concentrations of magnesium salts and limited amounts of potassium (K^+) and sodium (Na^+) salts," is obtained from seawater by precipitating other salts present in seawater such as $CaCO_3$, $CaSO_4$, and NaCl by solar evaporation. LB has many advantages as a coagulant: it can be produced on a large scale while maintaining cost effectiveness, it has a reduced application volume thus causing the least change to the suspension volume, it provides high fecal and total coliform removal efficiencies which reducing disinfection costs, and it yields high turbidity, TSS, and heavy metals removal efficiencies of highly turbid wastewater [11,13–17]. A drawback of using LB is the increased sludge volume [18]; yet, magnesium can be extracted from the sludge by dissolving $MgOH_2$, using CO_2, where the dissolved magnesium can be recycled several times and used as the precipitating coagulant [11]. The use of CO_2 to lower pH does not add to operating costs since it is used to lower the alkalinity of the effluent treated with LB prior to its discharge. [13].

Mixing conditions affect the average floc size distribution and, consequently, the efficiency of the coagulation–flocculation process. Shear is applied in two phases (fast and slow), each characterized by its own speed (shear rate, rpm) or average velocity gradient G (s^{-1}) and mixing time t (s). The nature of water to be treated, pH, and suspended solids (SS) concentration affect the optimum G and t values at which effective aggregation is achieved [1,4,5,12,19,20].

Optimum G and t values can be determined simultaneously where their product, Gt, known as the Camp number, gives a dimensionless number that can indicate the effectiveness of a coagulation–flocculation process. Determining the optimum G, t, and Gt values can be supported with residual turbidity measurements. Turbidity removal is an important factor used to investigate the state of aggregation since, microfloc structure and size distribution are the main parameters determining residual turbidity [8,9].

Fast mixing is a basic step in water and WWT, where the success of the coagulation–flocculation process highly depends on it [21]. Its main purpose is to equally disperse the coagulant into the suspension to incite efficient flocculation [20]. Fast mixing becomes more fundamental in case of highly turbid wastewater, where the higher particle collision rate due to the high-particle concentration will increase adsorption and floc formation rates [8,9].

Fast mix time has a great impact on floc formation during the slow mix phase [3]. In general, fast mixing for a time shorter than the optimum yields higher residual turbidity and larger flocs. Yu et al. [22] reported that a fast mix time of 10 s at 200 rpm fast mixing speed (50 rpm slow mixing speed for 10 min) was not sufficient for complete adsorption to take place, when applied to 50 mg/L kaolin clay suspension treated with alum as a coagulant. Yukselen and Gregory [3] showed that the stable flocculation index (FI) plateau value was achieved relatively quickly with higher FI values and lower residual turbidities for shorter fast mixing times (5 and 10 s compared with 30 s at 400 rpm) when adding alum to a 50 mg/dm^3 kaolin clay suspension.

As for fast mixing speed, many studies proved that turbidity removal is more efficient with higher fast mixing speed values. Kan et al. [8] tested the effect of fast mixing intensities 25, 80, 200, 350, and 600 s^{-1} applied to a 180 NTU reagent-grade clay suspension, aggregated by polyaluminum chloride PACl. Lowest residual turbidity (3.4 NTU) was achieved at $G = 350\ s^{-1}$. This implied that the increased intensity caused more small particles to flocculate.

Floc properties are not easy to characterize because of the irregularity of flocs' sizes and shapes [5,23]. Various methods have been applied to monitor different floc properties. Jarvis et al. [24] and Gregory [25] presented comprehensive reviews of methods used so far to study aggregation monitoring and control techniques including those measuring flocculation rate, particle count, and particle size. The photometric dispersion analyzer (PDA2000) used in this experimental study is an instrument that uses the transmission of a narrow beam of a high intensity light (850 nm wavelength) for continuous monitoring of flowing suspensions of various concentrations and particle sizes [4]. The transmitted light intensity has two components: a direct current (DC), corresponding to the average transmitted light; and the root mean square of the fluctuating transmitted intensity (RMS) [3]. The parameter used to study aggregation/disaggregation at constant concentration is the ratio of (DC/RMS), which is highly associated with floc size, and therefore, used as an indicator of aggregate formation. It is usually represented as FI such that FI increases with aggregation and decreases with disaggregation. At a constant applied shear, average floc size is a measurement of floc strength such that stronger flocs are considered more shear resistant and, thus, would have larger sizes [3–6,8,9,19,26–28].

Since little is known about the characteristics of flocs formed by the use of LB under different operating conditions, the presented work was conducted to characterize LB magnesium flocs under the effect of fast mixing conditions using an unique optical method, PDA, that has not been previously applied to LB flocs. Therefore, the main objectives were:

- To monitor and evaluate the effect of fast mixing shear rate and time on turbidity and TSS removal efficiencies, flocculation rate in addition to the strength, and size of flocs formed due to the use of LB as a coagulant in highly turbid kaolin clay suspensions.
- To optimize fast mixing conditions when LB is used as a coagulant on highly turbid waters.

2. Materials and methods

2.1. Kaolin clay suspension

Test water samples were prepared by dispersing 102 ± 9 g of powdered EPK kaolin clay (Edgar Minerals Inc., Florida, USA) in 42 L of deionized (DI) water to produce a suspension with an average turbidity of 1,213 ± 36 NTU. In order to retain the clay particles in suspension, the pH was raised and maintained at 7.5 by adding 5 M NaOH from a stock solution that was prepared by adding 20 g of NaOH pallets (HIMEDIA, India) to 100 mL of DI water and dissolving the same by the use of a magnetic stirrer. The suspension was mixed at 4,000 rpm for 40 min using a fast mixer (Barnant, Illinois, USA), mounted on top of a 45 L plastic container. The pH was continuously monitored throughout the mixing process using a pH meter (OAKTON Instruments, Illinois, USA) with NaOH added to the suspension, when needed to maintain the pH at 7.5 [3,22]. After allowing for overnight settling, 28 L of the supernatant was transferred to a glass tank for later use in the jar test. Two samples of the supernatant were collected to measure the initial TSS and turbidity.

2.2. Coagulant: liquid bittern

Liquid bittern (LB) was used as a coagulant in the experiment. LB was prepared from seawater during the period of the experiment using the method described by Ayoub et al. [14,15]. One sixty liters of seawater was emptied into two metal black-painted trays, mounted on the roof of the Raymond Ghosn Building at the American University of Beirut. The average physiochemical properties of the used LB are shown in Table 1. The optimum LB volume applied to 2 L of 1,213 ± 36 NTU suspension was found to be equivalent to 1072 mg Mg^{2+}.

2.3. Experimental setup and procedure

Coagulation–flocculation was carried in a B-KER® (Phipps and Bird, Virginia, USA) square, acrylic, 2-L testing jar (11.5 × 11.5 × 21cm) equipped with a 2.5 × 7.6 mm stainless steel flat paddle adjustable to a maximum depth of 23 cm and different speeds (maximum of 300 rpm). The G values (s^{-1}) corresponding to the different rotary speeds of the rotating flat paddle (rpm) applied throughout the experimental study were interpolated from Cornwell and Bishop [29].

The pH of the decanted 28 L of the 1,213 ± 36 NTU kaolin suspension was raised to 10.5 using the 5 M NaOH alkalizing solution, then 2 L of the suspension was transferred to one jar of the jar tester. Using a 3 mm internal diameter (ID) transparent Tygon tube, the suspension was conveyed from the jar through the flow cell of the PDA to the suction end of a peristaltic pump which was placed downstream of the jar tester and the PDA. The suspension exiting the flow cell was recycled back into the mixing jar at a rate of 25 ml/min through a Tygon tube connected to the outlet of the pump (Fig. 1). To maintain the temperature during the jar test, the jars were isolated using foam jackets, while the room temperature was maintained at 20 ± 1˚C. LB was added after fast mixing the suspension for 2 min and fast mixing conditions were varied according to Table 2. Preliminary experiments, using different combinations of slow mixing speed (20, 30, 40, and 50 rpm)

Table 1
Average physiochemical characteristics of the used liquid bittern

Parameter	Value
pH	6.47
Specific gravity	1.29
TDS (mg/L)	382,000
Conductivity (ms/cm)	92.5
Ca^{2+} (mg/LCa^{2+})	0
Mg^{2+} (mg/LMg^{2+})	68,770
Cl^{-} (mg/LCl^{-})	258,313
SO_4^{2-} mg/LSO_4^{2-}	54,500

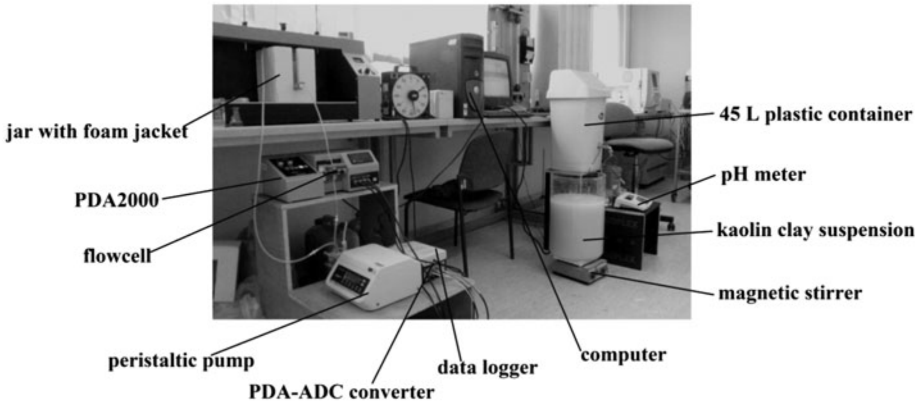

Fig. 1. Actual experimental setup.

Table 2
Variations of fast mixing speed and time

Time (s)	20	40	60
Speed (rpm)	80	100	120

and time (10, 20, and 30 min), were conducted to determine the optimum slow mixing conditions. Turbidity and TSS removal efficiencies, in addition to FI graphs, were compared and optimum slow mixing speed and time were found to be 20 rpm and 20 min, respectively, at which slow mixing was carried out. After the jar test was performed, the coagulated suspension was left to settle for 30 min. A 300 mL sample of the supernatant was carefully withdrawn to test for TSS and turbidity removal, in addition to change in pH. All experiments were repeated three times to ensure reproducibility of the results, and very little variation was observed. The ratio values recorded by the data logger were plotted as FI vs. time.

2.4. Parametric and statistical testing methods

The measured parameters included in this study were pH, temperature, turbidity, and TSS. These parameters were determined in accordance with the Standard Methods (APHA, 2011) SM 4500- H^+ B, SM2130 B, and SM 2540 D V 12,146, respectively, while the statistical methods used were the Anderson–Darling Normality Test for 95 and 99% confidence levels followed by one-way ANOVA (analysis of variance). Two multiple-comparison testing methods, namely Tukey's Honestly significant difference (HSD) test and Hsu's multiple comparisons with the best (MCB), were conducted to determine where the difference in means leading to null hypothesis rejection existed. Statistical tests were carried out using Minitab 16.

3. Results and discussion

3.1. Effect of fast mixing time

Optimum turbidity and TSS removal efficiencies were varied with both rapid mixing time and speed such that less fast mixing time was needed for higher speed values. Sixty seconds of fast mixing was required when the speed was 80 rpm; while 20 s was sufficient for optimum turbidity and TSS removal efficiencies at 120 rpm. When the suspension was mixed at 100 rpm, fast mixing time of 40 s yielded highest TSS and turbidity removal efficiencies (Fig. 2).

As fast mixing time did not have an impact on either the lag phase or flocculation rate, floc growth rate was the same for the different fast mixing periods (20, 40 and 60 s) at each fast mixing speed (80, 100, and 120 rpm) (Fig. 3). However, fast mixing time had a noticeable effect on the size and strength of the formed flocs. FI values were higher for shorter fast mixing times, such that the 20 s fast mixing time at various speeds (80, 100 and 120 rpm) resulted in largest flocs (Fig. 3), yet, it did not yield the strongest flocs. This was concluded by comparing the rates of decrease in FI in each set of experiments where for a constant shear rate, the least decrease in FI indicates stronger and more shear resistant flocs. This may indicate that the short fast mixing time did not allow for the equal dispersion of LB. Unequal distribution of the coagulant leads to the formation of "large coagulums," due to which magnesium hydroxide precipitate cannot sweep colloidal particles and adsorption–destabilization

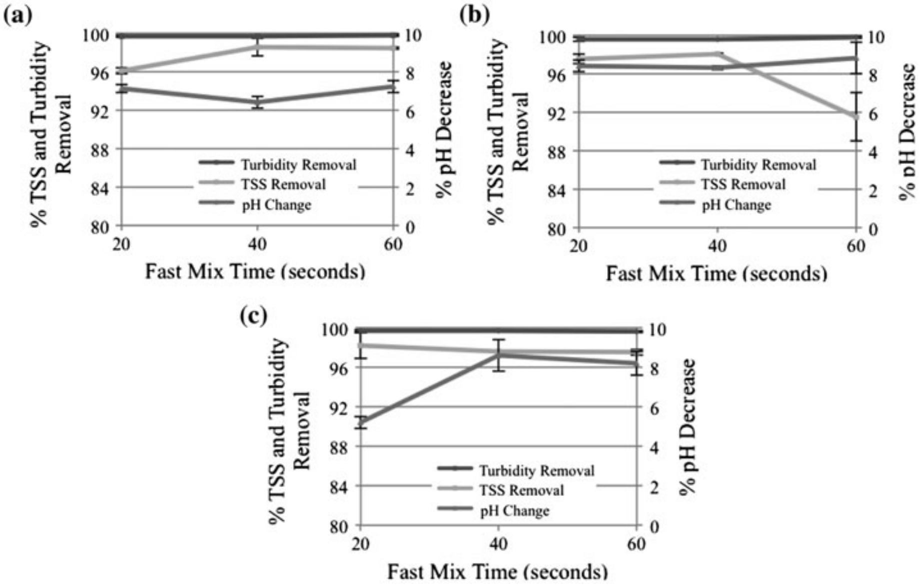

Fig. 2. Turbidity and TSS removal efficiencies and pH decrease in 20, 40, and 60 s fast mixing time at fast mixing speed of (a) 80 rpm, (b) 100 rpm, and (c) 120 rpm (Error bars represent ±1 standard deviation obtained from the three times repetition of every experiment).

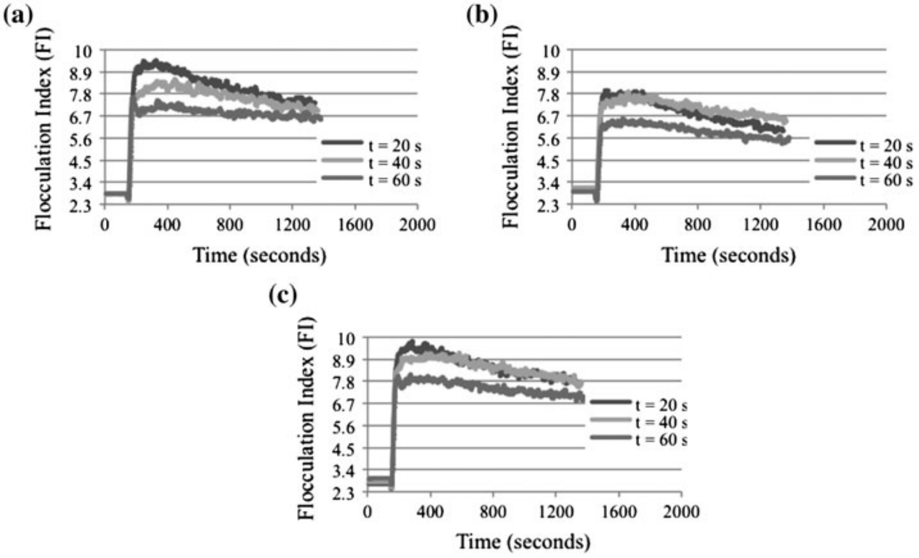

Fig. 3. FI graphs for 20, 40, and 60 s fast mixing time at fast mixing speed of (a) 80 rpm, (b) 100 rpm, and (c) 120 rpm.

mechanism would not be efficient enough to remove colloidal particles [21]. A 20 s mixing time was not sufficient to build shear resistant flocs and 60 s was needed for the formation of flocs whose FI reduced least with time (Fig. 3).

These results conform to several previous studies performed at different operating conditions. Yukselen and Gregory [3] reported that

> extended fast mix times give more limited floc growth, probably because, small and compact aggregates are formed during fast mixing, which lead to smaller flocs. With only brief periods of fast mixing there is less chance of compact aggregates being formed and more open, larger flocs can grow.

This study [3] showed that by applying 400 rpm followed by 10 min of slow mixing at 50 rpm to a 100

NTU kaolin clay suspension treated with alum, FI reached higher values for shorter fast mixing times where 5 and 10 s of fast mixing resulted in flocs much larger than those formed for 30 and 60 s of fast mixing. In another study by Yu et al. [22], the fast mix time was increased from 10 to 30 to 60 and 120 s at a 200 rpm mixing speed followed by 50 rpm slow mixing for 10 min of a 50 mg/L kaolin clay suspension using alum as a coagulant. It was reported that the FI values in the plateau phase decreased with increasing fast mix time which was explained in terms of lower collision efficiency of small flocs under the effect of longer high shear rate and floc breakage to a limiting size.

3.2. *Effect of fast mixing speed*

As noted earlier, turbidity and TSS removal efficiencies are not only dependent on fast mixing speed but also on fast mixing time such that higher fast mixing speeds were required for shorter mixing times. Fig. 4 shows that for 20 s of fast mixing, the highest turbidity and TSS removal efficiencies were obtained at 120 rpm (157 s^{-1}); but when the fast mixing time was extended to 40 and 60 s, 80 (85 s^{-1}) rpm was sufficient to yield the optimum turbidity and TSS removals. Rossini et al. [21] used lowest residual turbidity to correspond to optimum G and fast mixing speed was varied from 40 to 400 s^{-1} for 60 s fast mixing time. It was reported that as G was increased to 200 s^{-1}, after the addition of alum, the residual turbidity of tannery wastewater decreased from 500 to about 17 NTU and that was attributed to the fast hydrolysis of alum and the formation of aluminum hydroxide precipitates (7 s). So, increasing G enhanced the adsorption–destabilization processes. Unlike alum, iron hydroxide flocs were more susceptible to erosion under the effect of high shear such that primary particles forming the flocs failed to hold together.

Independent of its duration, fast mixing speed did not affect the lag time or slope of the rise phase. For all fast mixing times, 120 rpm caused the formation of largest flocs while 100 rpm yielded smallest flocs (Fig. 5). As fast mixing time was extended from 20 s to 40–60 s, the difference between floc sizes at different fast mixing speeds was diminished and relative floc sizes were closer to each other. This may indicate that the extension fast mixing time ensures enough successful collisions rather than fast mixing speed. Zouboulis and Traskas [6] indicated that for $G > G_{optimum}$, floc size reaches a limiting size. Also, the most shear resistant flocs corresponding to the least change in FI during slow mix phase are those formed after 60 s of fast mixing time for all fast mixing speed values (Fig. 5 (c)). This reassures the observation in Section 3.1, where at the same fast mix speed the flocs became stronger as the fast mixing time was extended from 20 to 40–60 s, enough time to restructure the aggregates composing the floc into a more compact shear resistant form. Shear does not always causes the

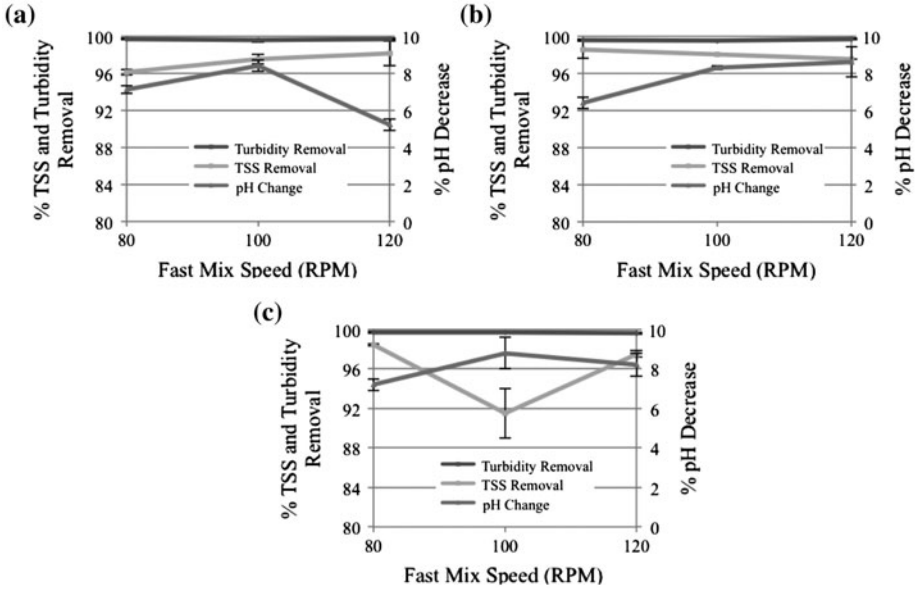

Fig. 4. Turbidity and TSS removal efficiencies and pH decrease in 80, 100, and 120 rpm fast mixing speed for fast mixing time of (a) 20 s, (b) 40 s, (c) 60 s (Error bars represent ±1 standard deviation obtained from the three times repetition of every experiment).

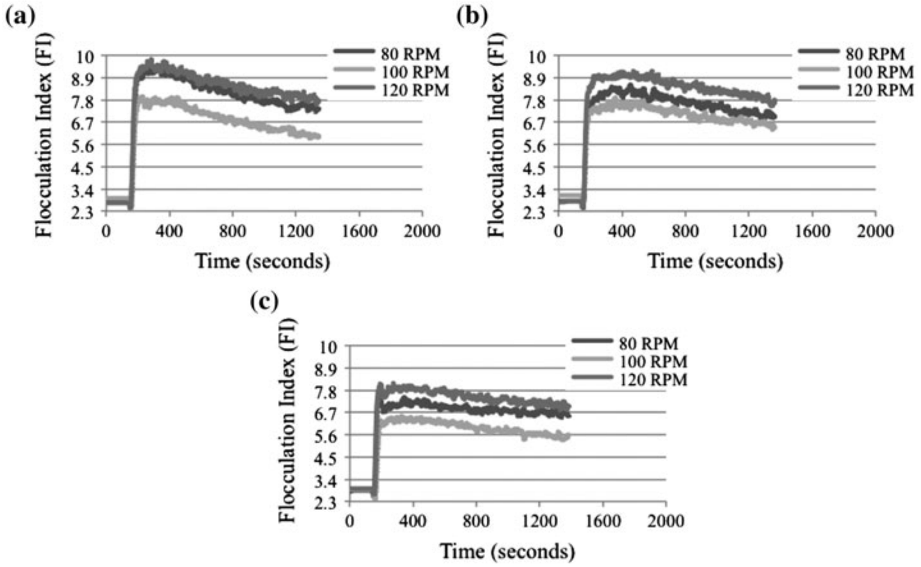

Fig. 5. FI graphs at 80, 100, and 120 rpm fast mixing speed for fast mixing time of (a) 20 s; (b) 40 s; and (c) 60 s.

breakdown of aggregates, but rather the re-organization of particles composing the floc, thus, causing it to be more compact [1].

3.3. Effect of fast mixing Gt value

Fast mixing *Gt* values were varied between 1,700 and 9,420. Turbidity removal efficiency maintained high values (always above 99%) for all Gt values. While TSS removal efficiency attained lower values, the best TSS removal efficiencies of 98–98.5% corresponded to fast mixing Gt values ranging between 3,140 and 5,100, with a sharp decrease in $Gt = 6{,}840$ at which TSS removal efficiency was 91.5% (Fig. 6). It was noted that higher turbidity and TSS removals did not necessarily correspond to highest pH decrease, which may indicate that enhanced turbidity and TSS removals were not due to the formation of more magnesium hydroxide but rather by better enmeshment of

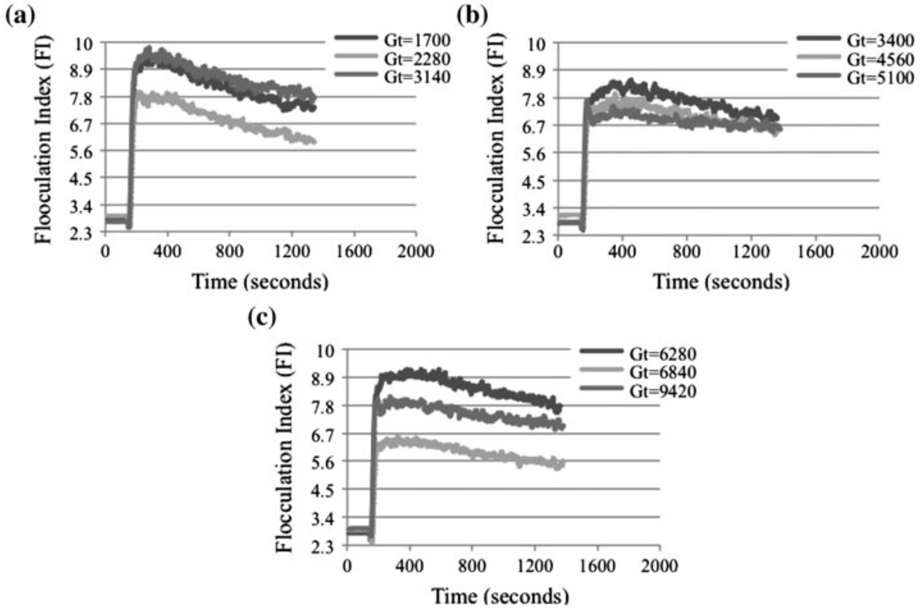

Fig. 6. FI graphs for Gt fast mixing values of (a) 1,700, 2,280, and 3,140; (b) 3,400, 4,560, and 5,100; (c) 6,280, 6,840, and 9,420 at 20 rpm slow mixing speed for 20 min (slow mixing $Gt = 16{,}800$).

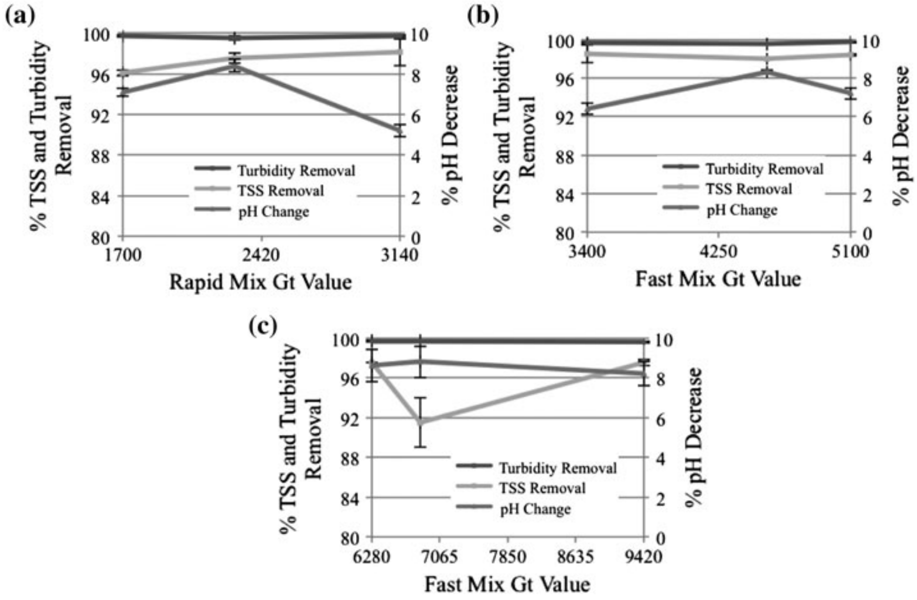

Fig. 7. Turbidity and TSS removal efficiencies and pH decrease in Gt fast mixing values of (a) 1,700, 2,280, and 3,140; (b) 3,400, 4,560, and 5,100; (c) 6,280, 6,840, and 9,420 at 20 rpm slow mixing speed for 20 min (slow mixing $Gt = 16,800$) (Error bars represent ±1 standard deviation obtained from the three times repetition of every experiment).

suspended and colloidal particles by the magnesium hydroxide precipitate.

The total Gt value had no effect on the lag and rise phases. Largest flocs were obtained at fast mixing Gt values 3,140 and 6,280 equivalent to 20 and 40 s fast mixing time, respectively, at 120 rpm. By comparing Fig. 7 (a)–(c), it was clear that for fast mixing Gt values 1,700–3,140, the flocs were weaker as indicated by the sharper decrease in FI values during the slow mix phase. Moreover, it was observed that flocs formed at fast mixing Gt values between 6,280 and 9,420 experienced least change in FI values, and consequently in their size, during the slow mixing phase. As shown before, these more shear resistant flocs corresponded to longer fast mixing time (40 and 60 s) (Fig. 7(b) and (c)).

4. Conclusions

Using high turbidity kaolin clay suspension (1,213 ± 36 NTU) and liquid bittern as a coagulant, the effects of fast mixing conditions on magnesium hydroxide floc formation rate and strength were studied in this paper. The following can be concluded:

- Shorter fast mixing time (20 s) produced larger magnesium flocs; yet, these was not the strongest and 60 s were required to build flocs that are more shear resistant during the slow mixing phase.
- The largest flocs were formed at 120 rpm fast mixing speed; however, the strength of the flocs was depended on the fast mix time rather than the speed where more shear resistant flocs were yielded for elongated fast mixing time (40 and 60 s) at different fast mixing speed values.
- Largest flocs were obtained at 120 rpm fast mixing speed applied for 20 s; yet, the most shear resistant flocs were those formed at 100 rpm applied for 60 s.
- Fast mixing Gt values ranging between 6,280 and 9,420 caused the formation of stronger LB flocs that were more resistant to slow mix shear equivalent to a Gt value of 16,800.

Acknowledgments

The authors would like to thank the Environmental Engineering Research Center at the American University of Beirut for providing all necessary equipment and assistance during the experimental work.

References

[1] P.T. Spicer, S.E. Pratsinis, J. Raper, R. Amal, G. Bushell, G. Meesters, Effect of shear schedule on particle size, density, and structure during flocculation in stirred tanks, Powder Technol. 97 (1998) 26–34.
[2] A.T. Hubbard, Fine Clay Floccuation, Encyclopedia of Surface and Colloid Science, Marcel Dekker, New York, NY, 2002, pp. 2197–2206.

[3] M.A. Yukselen, J. Gregory, The effect of rapid mixing on the break-up and reformation of flocs, J. Chem. Technol. Biotechnol. 79 (2004) 782–788.

[4] T. Liu, Z. Chen, W. Yu, J. Shen, J. Gregory, Effect of two-stage coagulant addition on coagulation–ultrafiltration process for treatment of humic-rich water, Water Res. 45 (2011) 4260–4268.

[5] P. Jarvis, B. Jefferson, J. Gregory, S.A. Parsons, A review of floc strength and breakage, Water Res. 39 (2005) 3121–3137.

[6] A.I. Zouboulis, G. Traskas, Comparable evaluation of various commercially available aluminium-based coagulants for the treatment of surface water and for the post-treatment of urban wastewater, J. Chem. Technol. Biotechnol. 80 (2005) 1136–1147.

[7] W. Yu, J. Gregory, L. Campos, Breakage and regrowth of Al-Humic flocs—Effect of additional coagulant dosage, Environ. Sci. Technol. 44 (2010) 6371–6376.

[8] C. Kan, C. Huang, J.R. Pan, Coagulation of high turbidity water: The effects of rapid mixing, J. Water Supply: Res. Technol. 51(2) (2002) 77–85.

[9] C. Kan, C. Huang, J.R. Pan, Time requirement for rapid-mixing in coagulation, Colloids Surf., A 203 (2002) 1–9.

[10] M.A. Yukselen, J. Gregory, The reversibility of floc breakage, Int. J. Miner. Process. 73 (2004) 251–259.

[11] J. Zhao, W. Lin, Q. Chang, W. Liu, S. Wang, Y. Lai, Effects of operational conditions on the floc formation time and rate in magnesium hydroxide coagulation process, Desalin. Water Treat. 45 (2012) 153–160.

[12] I. Solomentseva, S. Bárány, J. Gregory, The effect of mixing on stability and break-up of aggregates formed from aluminum sulfate hydrolysis products, Colloids Surf., A 298 (2007) 34–41.

[13] G.M. Ayoub, F. Merehbi, R. Abdallah, A. Acra, M. El Fadel, Coagulation of alkalinized municipal wastewater using seawater bittern, Water Environ. Res. 71 (1999) 443–453.

[14] G.M. Ayoub, M. El-Fadel, A. Acra, R. Abdallah, Critical density index for the solar production of bittern from seawater, Int. J. Environ. Stud. 58 (2000) 85–97.

[15] G.M. Ayoub, F. Merhebi, A. Acra, M. El Fadel, B. Koopman, Seawater bittern for the treatment of alkalized industrial effluents, Water Res. 34 (2000) 640–656.

[16] G.M. Ayoub, L. Semerjian, A. Acra, M. Fadel, B. Koopman, Heavy metal removal by coagulation with seawater liquid bittern, J. Environ. Eng. 127 (2001) 196–207.

[17] L. Semerjian, G.M. Ayoub, High-pH-magnesium coagulation–floccualtion in wastewater treatment, Adv. Environ. Res. 7 (2003) 389–403.

[18] G.M. Ayoub, F. Merhebi, Characteristics and quantities of sludge produced by coagulating wastewater with seawater bittern, lime and caustic, Adv. Environ. Res. 6 (2002) 277–284.

[19] T. Li, Z. Zhu, D. Wang, C. Yao, H. Tang, Characterization of floc size, strength and structure under various coagulation mechanisms, Powder Technol. 168 (2006) 104–110.

[20] W. Sheng, X.F. Peng, D.J. Lee, A. Su, Coagulation of particles through rapid mixing, Drying Technol. 24 (2006) 1271–1276.

[21] M. Rossini, J. Garcia Garrido, M. Galluzzo, Optimization of the coagulation–flocculation treatment: Influence of rapid mix parameters, Water Res. 33 (1999) 1817–1826.

[22] W. Yu, J. Gregory, L. Campos, G. Li, The role of mixing conditions on floc growth, breakage and re-growth, Chem. Eng. J. 171 (2011) 425–430.

[23] B. Jefferson, P. Jarvis, E. Sharp, S. Wilson, S.A. Parsons, Flocs through the looking glass, Water Sci. Technol. 50 (2004) 47–54.

[24] P. Jarvis, B. Jefferson, S. Parsons, Measuring floc structural characteristics, Rev. Environ. Sci. Bio/Technol. 4 (2005) 1–18.

[25] J. Gregory, Monitoring particle aggregation processes, Adv. Colloid Interface Sci. 147–148 (2009) 109–123.

[26] J. Gregory, Monitoring floc formation and breakage, Water Sci. Technol. 50 (2004) 163–170.

[27] W. Xu, B. Gao, Q. Yue, X. Bo, Influence of pH on flocs formation, breakage and fractal properties- the role of Al13 polymer, J. Water Sustainability 1 (2011) 45–57.

[28] Photometric Dispersion Analyser PDA2000 Operating Manual. Rank Brothers, Cambridge.

[29] D.A. Cornwell, M.M. Bishop, Determining velocity gradients in laboratory and full-scale systems, Res. Technol. 75 (1983) 470–475.